Malaysian Journal of Chemistry, 2025, Vol. 27(3), 134-148
(Special Issue: *2nd International Science and Technology Colloquium, i-COSTECH 2024*)

Adsorptive Removal of Methylene Blue using Activated Carbon Derived from Waste Coffee Grounds

Muhammad Adam Danial Mohd Yusri and Zaidi Ab Ghani*
Faculty of Applied Sciences,
Universiti Teknologi MARA Cawangan Perlis, 02600 Arau, Perlis, Malaysia
*Corresponding author (e-mail: zaidi433@uitm.edu.my)

In this work, activated carbon derived from waste coffee grounds (CG-AC) was synthesized using zinc chloride ($ZnCl_2$) as the activating agent. The CG-AC was then employed as an adsorbent for the removal of methylene blue (MB) from aqueous solutions. Adsorption isotherm data were evaluated using the Langmuir, Freundlich, and Temkin models. The Langmuir model, with a correlation coefficient of 0.9998, showed the best fit for the adsorption of MB on CG-AC, with the maximum monolayer adsorption capacity calculated at 176 mg/g. Kinetic studies were conducted using pseudo-first-order (PFO), pseudo-second-order (PSO), and intraparticle diffusion (IPD) models. The R^2 values indicated that the PSO model provided a more accurate description of the adsorption kinetics. The plot of q_t versus $t^{1/2}$ in the IPD model demonstrated multi-linear behavior, suggesting that the adsorption occurred in multiple stages. Thermodynamic analysis was performed at temperatures ranging from 25 to 34 °C, where negative $\Delta G°$ values and positive $\Delta H°$ values confirmed the spontaneity and endothermic nature of the adsorption process. Additionally, the positive $\Delta S°$ value indicated a strong affinity of MB molecules for the CG-AC. These results suggest that CG-AC could be a promising adsorbent for treating wastewater containing high levels of dyes.

Keywords: Adsorption; methylene blue; activated carbon; isotherm; kinetic

Received: September 2024; Accepted: December 2024

Methylene blue (MB), a common azo dye with the molecular structure $C_{16}H_{18}ClN_3S$, is widely used as a coloring agent in various industries, such as textiles, leather, and paper production. Its presence in wastewater contributes to significant organic contamination, as many dyes, including methylene blue, are refractory and highly soluble. Exposure to methylene blue can result in adverse health effects, including dizziness, nausea, vomiting, perspiration, and mental disorientation [1].

Treating dye-contaminated wastewater is essential before environmental discharge, as even minimal concentrations (less than 1 mg/L) can visibly impair water quality. Several techniques are available to remove dyes from wastewater, such as filtration, flotation, adsorption, and photocatalysis [2]. Of these, adsorption onto porous materials stands out for its effectiveness, cost-efficiency, simplicity, and eco-friendliness, making it a promising approach for water purification [3].

Adsorption is a surface-based phenomenon involving the attachment of particles to an adsorbent's surface via chemical or physical bonds. Researchers have explored various adsorbents for wastewater treatment, including activated carbon, natural clay, chitosan composites, nanoparticles, polymer-based adsorbents, and magnetic materials [4, 5]. Activated carbon, in particular is widely preferred due to its large surface area, high adsorption capacity, and cost-effectiveness. However, many conventional adsorbents face limitations, such as low diffusion rates, high costs, or the risk of secondary pollution. Practical, low-cost adsorbents with high efficiency and minimal environmental impact are therefore preferred for sustainable applications.

Despite the extensive use of activated carbon, gaps remain in understanding how operational factors influence the adsorption process for methylene blue removal. Key factors, such as pH, initial concentration, temperature, and contact time, as well as adsorption isotherms, kinetic models, and thermodynamic parameters, require a comprehensive investigation to enhance the effectiveness of adsorption processes.

To address these gaps, this study aims to optimize methylene blue adsorption by evaluating the effects of pH, initial concentration, temperature, and contact time on activated carbon's adsorption efficiency. Additionally, this research explores adsorption isotherms, kinetic models, and

---

†Paper presented at the 2nd International Science and Technology Colloquium (i-COSTECH 2024)

thermodynamic parameters to deepen understanding of the adsorption mechanism and improve wastewater treatment methods.

EXPERIMENTAL

Chemicals and Materials

In this study, the adsorbent utilized was CG-AC, which was prepared from waste coffee grounds and activated using $ZnCl_2$ (Sigma-Aldrich, USA). Unless stated otherwise, all chemicals used were of analytical reagent grade and purchased from Sigma-Aldrich, USA. The adsorbate employed was MB, a cationic dye (Merck, Germany). MB adsorption data were used to derive adsorption isotherms and to conduct kinetic and thermodynamic studies. A stock solution of MB (1000 mg/L) was prepared by dissolving 1 g of MB in 1 L of distilled water. This stock solution was subsequently diluted with distilled water to achieve the desired concentrations of MB ranging from 50 to 200 mg/L.

Batch Adsorption Methods

A batch adsorption method was utilized to study the removal of MB from aqueous solutions using CG-AC. To evaluate the effect of adsorbent dosage, varying amounts of CG-AC, from 0.02 to 0.20 g, were introduced into 250 mL Erlenmeyer flasks containing 100 mL of MB solution with a concentration of 100 mg/L. The impact of the initial MB concentration was analyzed by using seven concentrations, ranging from 100 to 200 mg/L. Contact time was monitored from the beginning of the experiment until equilibrium was reached, spanning from 15 to 150 minutes. The solution pH was adjusted from 4.5 to 9.0 to evaluate its effect on MB adsorption. The effect of temperature was examined within the range of 25 to 34 °C while keeping all other parameters constant. This temperature range reflects typical ambient conditions found in wastewater treatment applications and aligns with temperatures used in related studies. The samples were agitated at room temperature at 175 rpm using an orbital shaker. After shaking, the mixtures were filtered to remove any remaining adsorbent particles before analysis. The MB content in the filtered solutions was measured using a UV-visible spectrophotometer at a wavelength of 664 nm, which corresponds to the maximum absorption peak of MB. The adsorption capacity of MB was calculated using Equation (1) as follows:

$$q_e = [(C_o - C_e)\ V]\ /\ M \qquad (1)$$

In this context, C_e (mg/L) and C_o (mg/L) represent the equilibrium and initial concentrations of the adsorbate, respectively. The mass of the adsorbent is denoted as M (g), while V (L) refers to the volume of the solution. Isotherm parameters for the Langmuir, Freundlich, and Temkin models were evaluated using experimental adsorption data from various initial concentrations of C_o. For kinetic experiments, the procedure was similar to that described above, with approximately 2 mL of MB solution withdrawn at predetermined time intervals using a syringe. The MB concentration in the solution (C_t, mg/L) was measured over time, and the adsorption capacity (q_e) was calculated according to Equation (2):

$$q_t = [(C_o - C_t)\ V]\ /\ M \qquad (2)$$

In this equation, q_t is the amount of MB adsorbed per unit mass of adsorbent at time (mg/g), C_o and C_t are the initial and time-dependent concentrations of the adsorbate solution (mg/L), respectively. The solution volume is represented as V (L), and M refers to the mass of the adsorbent used (g). Thermodynamic analysis followed a procedure similar to that used for the adsorption equilibrium study, with temperatures ranging from 24 to 34 °C. The CG-AC dosage and MB concentration were maintained at 0.10 g and 100 mg/L, respectively. The adsorption capacity of MB in the aqueous phase was calculated using Equation (1). Experimental data for the isotherm, kinetic and thermodynamic analysis were fitted to their respective linear equations, as shown in **Table 1**.

RESULTS AND DISCUSSION

Batch Adsorption Study

This section outlines the findings related to the removal of MB from aqueous solutions using a batch process with CG-AC as the adsorbent. The study examines the effects of several process parameters, such as adsorbent dosage, initial dye concentration, contact time, pH, and temperature, to determine the optimal conditions for enhancing removal efficiency. The results from these batch experiments are detailed in the subsequent sections.

Table 1. Equations of isotherm models, kinetics, and thermodynamic study.

Parameters	**Equation**	
Langmuir	$C_e/q_e = 1/bq_m + C_e/q_m$; $R_L = 1/(1+ bC_o)$	(3)
Freundlich	$\text{In } q_e = \text{In } K_F + (1/n) \text{ In } C_e$	(4)
Temkin	$q_e = B \text{ In } K_T + B \text{ In } C_e$ $B = RT/b_T$	(5)
Pseudo-first order (PFO)	$\text{In } (q_e - q_t) = \text{In } q_e - K_1 t$	(6)
Pseudo-second order (PSO)	$t/q_t = (1/k_2 q_e^2) + (1/q_e)\, t$	(7)
Intraparticle diffusion (IPD)	$q_t = k_{ID} t^{0.5} + C_i$	(8)
Thermodynamic	$\text{In}K_D = -\Delta G^o/RT$ $\text{In}K_D = (\Delta S^o/ R) - (\Delta H^o / RT)$; $\Delta G^o = \Delta H^o - T\Delta S^o$	(9)

Note:

q_e = amount of adsorbate at equilibrium (mg/g)
q_t = amount of adsorbate retained at time (mg/g)
q_m = monolayer capacity of the adsorbent (mg/g)
t = time (min)
k_1 = PFO rate constant (1/min)
k_2 = PSO rate constant (g/mg.min)
k_{ID} = IPD rate constant (mg/g/min$^{0.5}$)
C_i = thickness of the boundary layer (mg/g)
b = Langmuir adsorption equilibrium constant (L/mg)
C_e = equilibrium concentration (mg/L)
C_o = initial concentration (mg/L)
R_L = separation factor
n = adsorption intensity
K_F = constant relating to the adsorption capacity (L/g)
K_T = Temkin equilibrium binding constant (L/g)
b_T = Temkin isotherm constant (mg/L)
R = gas constant (8.314 J/mol.K)
T = absolute temperature (K)
q_s = theoretical saturation capacity (mg/g)
k_D = adsorption equilibrium constant (l/mg)
$\Delta G°$ = free energy (kJ/mol)
$\Delta S°$ = change in enthalpy (kJ/mol)
$\Delta H°$ = change in entropy (J/mol.K)

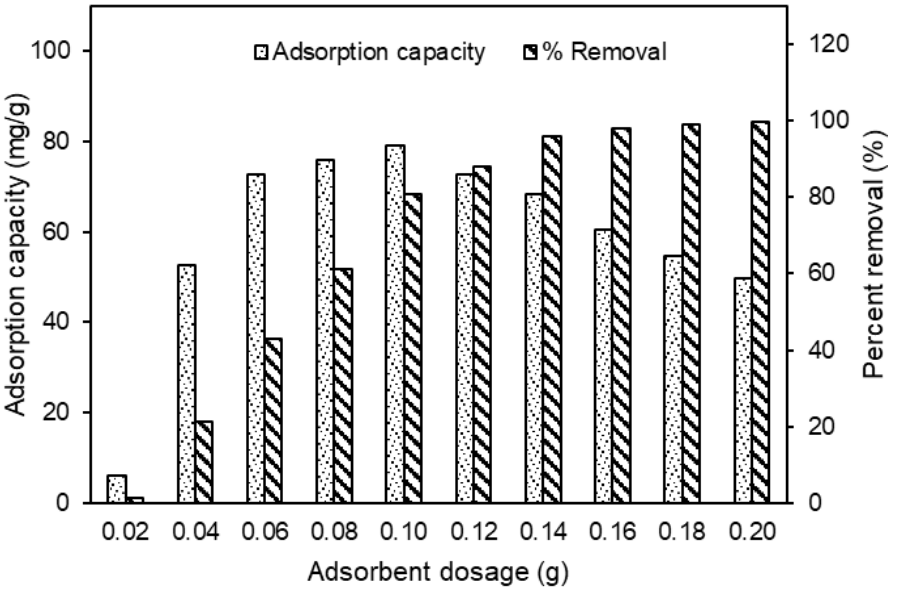

Figure 1. Effect of adsorbent dosage on adsorption capacity and percent removal of MB (MB dye concentration = 100 mg/L, adsorbent dose = 0.2-2.0 g/L, solution pH = 8.0, volume of the sample = 100 mL, and time = 60 minutes).

Effect of Adsorbent Dosage

The effect of adsorbent dosage on methylene blue (MB) removal was investigated by varying activated carbon (AC) dosage from 0.02 g to 0.20 g in a constant 100 ppm MB solution, as shown in **Figure 1**. Results demonstrated a significant increase in removal efficiency, rising from 1.31% to 99.60% with higher AC dosages. This improvement is due to the increased availability of active adsorption sites as more AC is introduced, providing a greater surface area for dye molecule interaction. These findings are consistent with Deivasigamani et al. [6], who observed that higher adsorbent dosages enhance removal efficiency by increasing the total adsorption surface area.

However, the adsorption capacity decreases as dosage increases, since the same quantity of dye molecules is distributed across a larger adsorbent surface. This results in a lower specific adsorption capacity, despite overall efficiency gains. Mani et al. [7] also noted that while higher AC dosages improve dye removal rates, they dilute the adsorption sites relative to dye concentration, reducing q_e. Similarly, Deivasigamani et al. [6] reported that at higher adsorbent dosages, adsorption efficiency improves, but the proportional decrease in q_e suggests diminishing returns for excessive dosages. These findings emphasize the trade-off between removal efficiency and specific adsorption capacity. Ouaddari et al. [8] highlighted the importance of optimizing adsorbent dosage to balance removal efficiency and cost-effectiveness. Excessive dosages may result in higher operational costs without substantial improvements in dye removal. Thus, determining an optimal dosage is essential to achieve efficient and economical dye removal.

In conclusion, increasing AC dosage significantly enhances MB removal efficiency by providing more adsorption sites, though it reduces the specific adsorption capacity per gram. Identifying the optimal adsorbent dosage is critical to ensure effective and cost-efficient dye removal processes. This balance prevents resource overuse while maximizing adsorption performance, aligning with both economic and environmental sustainability goals.

Effect of Initial Concentration

Figure 2 shows the effect of initial concentration on the adsorption of MB by CG-AC, with concentrations ranging from 100 to 200 mg/L. At 100 mg/L, the removal efficiency peaked at 99%, but it declined with increasing concentration. This trend aligns with common adsorption behavior, where higher initial concentrations result in greater adsorption capacity but reduced efficiency due to the saturation of active adsorption sites. At lower concentrations, abundant active sites on the AC surface allow for efficient adsorption of dye molecules. As concentration increases, the driving force for adsorption intensifies, leading to higher initial adsorption rates, as observed by Daniel et al. [9]. However, as the adsorbent surface becomes saturated, fewer active sites remain available, leading to a decline in removal efficiency. This phenomenon, known as "adsorption saturation," was similarly noted by Chen et al. [10], who reported that higher adsorbate concentrations accelerated the saturation of adsorbent surfaces, limiting further adsorption.

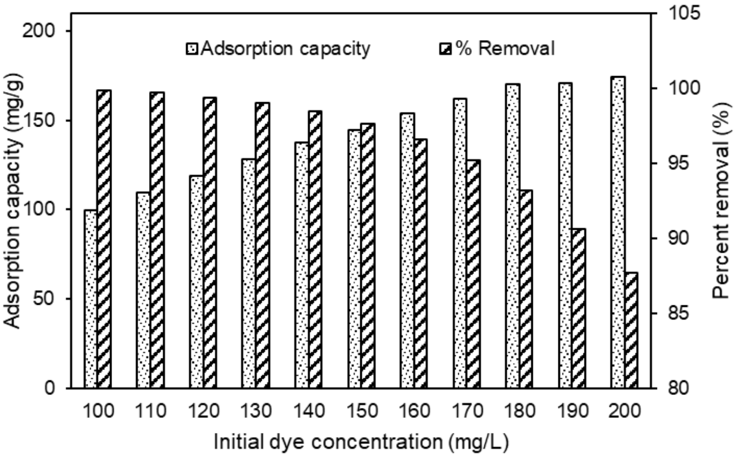

Figure 2. Effect of initial concentration on adsorption capacity and percent removal of MB (MB dye concentration = 100–200 mg/L, adsorbent dose = 1 g/L, solution pH = 8.0, volume of the sample = 100 mL, and time = 60 minutes).

The increase in adsorption capacity at higher concentrations reflects better utilization of the adsorbent's surface area, especially during the initial stages of adsorption. Daniel et al. [9] observed rapid dye uptake early in the process, which slows as active sites are occupied. At higher concentrations, competition for limited adsorption sites increases, reducing overall efficiency. This behavior is consistent with adsorption models such as Langmuir and Freundlich, which describe a saturation point beyond which increases in dye concentration do not proportionally enhance adsorption efficiency. Similar finding was reported by Mani et al. [7], who observed decreased efficiency at higher MB concentrations due to the exhaustion of available active sites.

In conclusion, the adsorption of MB onto AC is strongly influenced by initial concentration. While adsorption capacity increases with higher concentrations due to greater dye availability, removal efficiency decreases as the adsorbent surface becomes saturated. These results align with established adsorption mechanisms and emphasize the importance of optimizing dye concentration for efficient adsorption processes.

Effect of Contact Time

The results in **Figure 3** highlight the effect of contact time on MB adsorption efficiency using CG-AC. The adsorption capacity and percentage removal of MB increases significantly during the first 75 minutes, after which the removal rate slows, approaching equilibrium. This two-phase adsorption behavior involves an initial rapid phase followed by a slower, steady phase, consistent with typical adsorption processes. The initial phase, characterized by high adsorption rates, occurs due to the abundance of available adsorption sites on the activated carbon surface. During this period, dye molecules diffuse quickly from the bulk solution onto the external surface of the adsorbent, driven by the concentration gradient. Ouaddari et al. [8] reported similar rapid adsorption rates in dye removal studies, attributing this to external surface interactions between the adsorbate and adsorbent.

As contact time extends beyond 75 minutes, the adsorption rate decreases, indicating the saturation of external adsorption sites. Subsequently, dye molecules begin migrating into the internal pores of the activated carbon, where adsorption occurs at a slower rate due to intraparticle diffusion. This transition from surface adsorption to pore diffusion aligns with findings by Kim and Kim [11], who noted that intraparticle diffusion becomes the rate-limiting step in later stages of adsorption. Moreover, prolonged contact times enable deeper penetration of dye molecules into the activated carbon's porous structure, enhancing overall adsorption. Iqajtaoune et al. [12] observed that extended contact times improve the accessibility of internal adsorption sites, resulting in increased adsorption capacity. However, beyond optimal contact time, further increases in time provide minimal additional benefits, as equilibrium is reached. These results are consistent with Ouaddari et al. [8], who emphasized the importance of identifying an optimal contact time for efficient adsorption processes. The observed optimal contact time of 75 minutes in this study underscores the balance between rapid external surface adsorption and slower internal pore diffusion.

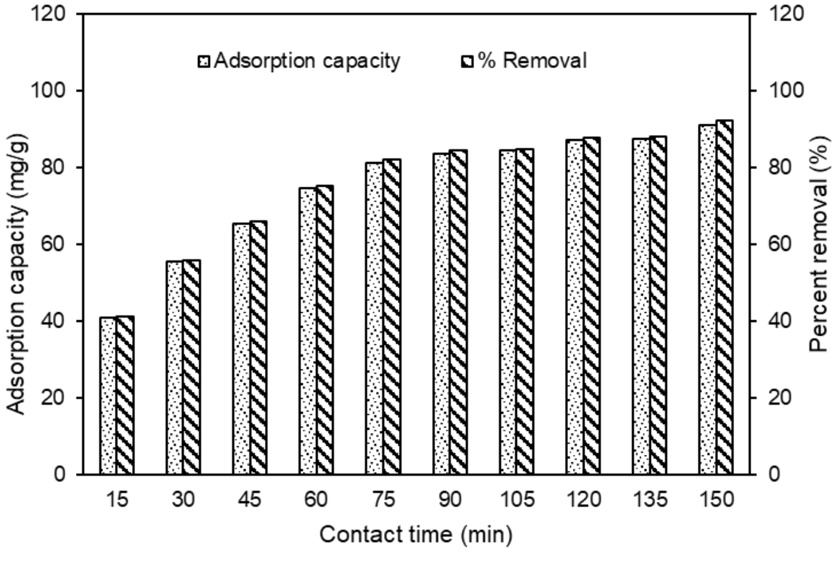

Figure 3. Effect of contact time on adsorption capacity and percent removal of MB (MB dye concentration = 100 mg/L, adsorbent dose = 1 g/L, solution pH = 8.0, volume of the sample = 100 mL, and time = 15-150 minutes).

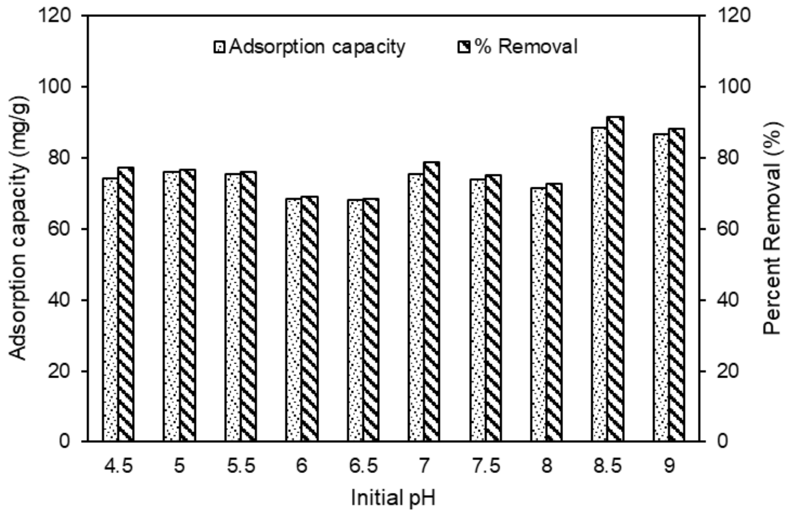

Figure 4. Effect of initial pH on adsorption capacity and percent removal of MB (MB dye concentration = 100 mg/L, adsorbent dose = 1 g/L, solution pH = 4.5-9.0, volume of the sample = 100 mL, and time = 60 minutes).

In conclusion, the study confirms that CG-AC achieves optimal adsorption efficiency within 75 minutes, driven by rapid initial diffusion and slower pore diffusion. This behavior reflects the typical dynamics of dye adsorption processes and highlights the critical role of both external and intraparticle diffusion.

Effect of pH

The pH of the MB solution significantly influences the adsorption process, as illustrated in **Figure 4**. The highest removal efficiency for MB was recorded at pH 8.5 (87.99%), with efficiency decreasing at both lower and higher pH values. This behavior highlights the intricate relationship between adsorbent surface charge, solution chemistry, and dye molecule properties during adsorption. At lower pH values, the removal efficiency declines due to the protonation of the activated carbon surface. Increased hydrogen ion concentration neutralizes the negatively charged functional groups on the carbon surface, reducing the electrostatic attraction between the positively charged MB molecules and the adsorbent. This is consistent with findings by Mani et al. [7], who observed similar trends in the adsorption of cationic dyes, where protonation of adsorbent surfaces inhibited dye adsorption at low pH.

Interestingly, the results of this study suggest an abnormal trend at lower pH levels, possibly indicating that the activated carbon surface became positively charged. In such cases, adsorption may occur via hydrogen bonding or van der Waals forces rather than electrostatic interactions. This phenomenon has been reported in studies by Wardighi et al. [13], who highlighted that hydrogen bonding and dispersion forces can dominate when the conventional electrostatic attraction is unfavorable. As pH increases towards 8.5, the negatively charged adsorption sites become more available due to deprotonation, enhancing the electrostatic attraction between MB and the activated carbon. Additionally, hydrogen bonding between functional groups on the activated carbon surface and MB molecules may further improve adsorption. Such observations align with studies by Iqajtaoune et al. [12], who reported optimal MB removal in alkaline conditions due to enhanced adsorbate-adsorbent interactions. However, at pH levels above the point of zero charge (pH_{pzc}), the presence of excess OH^- ions can disrupt adsorption by competing with MB molecules for active sites. This competition weakens the overall removal efficiency, as observed by Ouaddari et al. [8]. This underscores the necessity of optimizing solution pH to maximize adsorption efficiency.

In conclusion, the effect of pH on MB removal is governed by a combination of electrostatic forces, hydrogen bonding, and van der Waals interactions. Optimal adsorption occurs at slightly alkaline pH, while extreme pH values reduce efficiency due to either surface protonation or competition with hydroxyl ions. These findings emphasize the critical role of pH in designing effective adsorption systems.

Effect of Temperature

Figure 5 demonstrates the effect of temperature on the removal of MB using CG-AC. Adsorption capacity and percent removal increased from 25 °C to 34 °C. This trend suggests that adsorption is temperature-sensitive, with higher temperatures enhancing the adsorption process. The increased adsorption efficiency can be attributed to the enhanced mobility and diffusion of dye molecules, leading to improved interaction between the dye and the adsorbent surface. The endothermic nature of the adsorption process is evident from the results, as higher temperatures increase the kinetic energy of MB molecules, facilitating their movement towards active adsorption sites. Kim and Kim [11] reported a similar positive correlation between temperature and adsorption capacity, where elevated temperatures enhanced the penetration of dye molecules into the adsorbent's pores. This behavior aligns with findings by, who observed that higher temperatures improve both diffusion rates and chemical interactions, contributing to greater adsorption efficiency.

As the temperature increases, the rate of diffusion of the adsorbate molecules across the external boundary layer and in the internal pores of the adsorbent particles increase due to the decrease in the viscosity, leading to a higher dye uptake [14]. This aligns with Ouaddari et al. [8], who observed similar trends in methylene blue adsorption using natural and purified clays. They noted that increased temperatures enhanced the mobility of dye molecules, resulting in better interaction with the adsorbent and higher adsorption capacities. The results of this study corroborate previous findings, highlighting that adsorption processes benefit from increased molecular movement and collision frequency at elevated temperatures. These factors enable dye molecules to overcome energy barriers, facilitating penetration into the activated carbon's porous structure. From an application perspective, the observed improvement in adsorption efficiency at higher temperatures has practical implications for optimizing dye removal processes in industrial wastewater treatment. Temperature control can be a critical parameter to enhance adsorption performance.

In conclusion, the adsorption of methylene blue onto activated carbon is an endothermic process influenced significantly by temperature. Elevated temperatures enhance dye mobility, diffusion, and interaction with the adsorbent, leading to improved adsorption capacities. These findings are consistent with previous studies and underline the importance of temperature in designing efficient adsorption systems for industrial applications.

Adsorption Isotherm and Kinetic Study

The adsorption isotherm is used to assess the maximum adsorption capacity. Batch equilibrium isotherm curves depict the adsorption processes and can be represented by either mechanistic or empirical equations. While mechanistic models provide explanations, descriptions, and predictions of experimental outcomes, empirical models may fail to accurately reflect the experimental curves [15]. To fit the batch equilibrium isotherm curves, an empirical model that incorporates a limited number of parameters is utilized. The most commonly used models are the Langmuir and Freundlich models, which have demonstrated a high degree of success [16]. The adsorption isotherm represents the relationship between the amount of dye adsorbed (q_e) and the aqueous concentration (C_e) at equilibrium. To obtain the equilibrium data, the initial concentration of methylene blue was varied, while the amount of adsorbent in each sample was maintained at a constant 0.1 g.

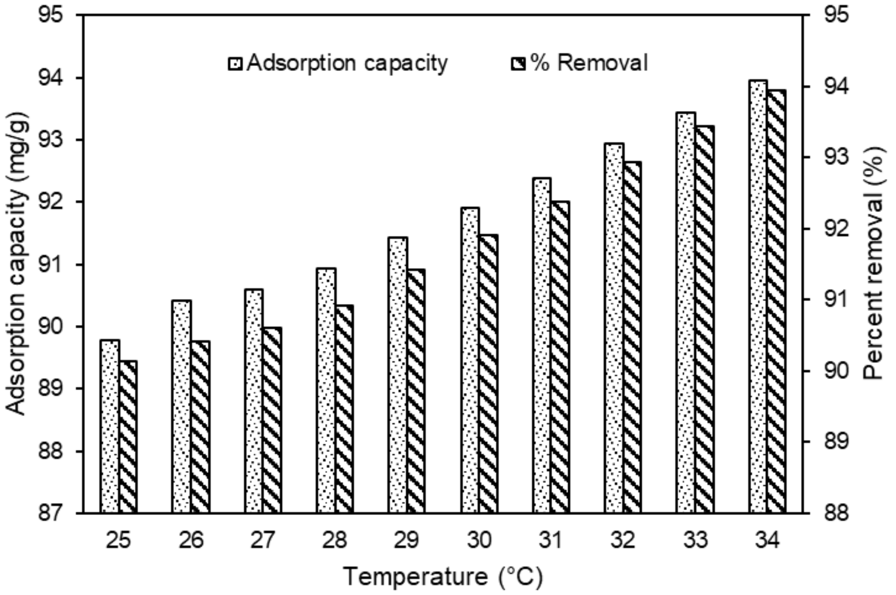

Figure 5. Effect of temperature on adsorption capacity and percent removal of MB (MB dye concentration = 100 mg/L, adsorbent dose = 1 g/L, solution pH = 8.0, volume of the sample = 100 mL, and time = 60 minutes).

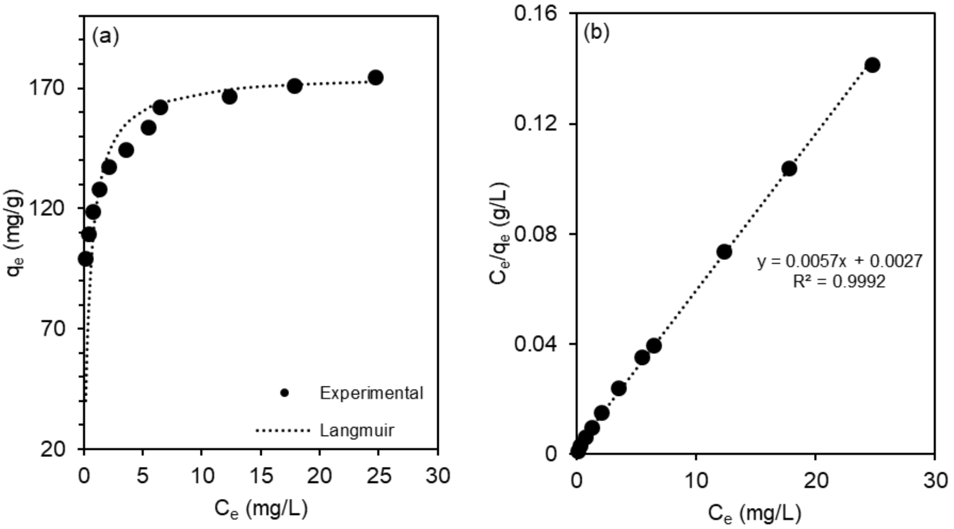

Figure 6. (a) Langmuir and (b) Linear Langmuir isotherm model for adsorption MB onto CG-AC.

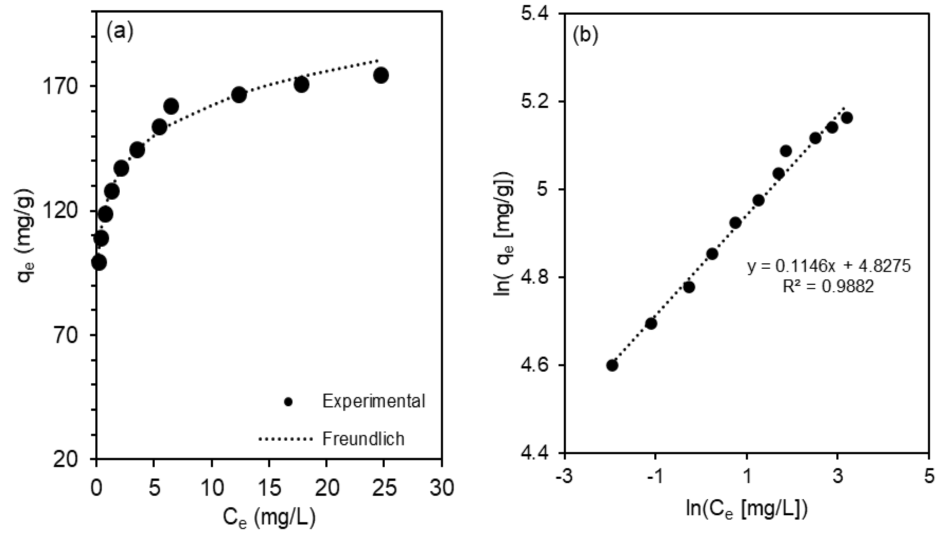

Figure 7. (a) Freundlich and (b) Linear Freundlich isotherm model for adsorption MB onto CG-AC.

Adsorption Isotherm

The Langmuir isotherm model assumes uniform adsorption sites on the adsorbent surface and a monolayer adsorption process where each binding site can hold only one adsorbate molecule, with no interactions between adsorbed molecules. **Figure 6(a)** illustrates the nonlinear Langmuir isotherm, showing the equilibrium concentration of MB (C_e) plotted against the adsorption capacity at equilibrium (q_e). The curve demonstrates saturation behavior, where q_e increases with C_e until the adsorption capacity reaches a maximum value (q_{max}), beyond which no further adsorption occurs, indicating monolayer coverage. This saturation point reflects the finite number of adsorption sites on CG-AC. **Figure 6(b)** represents the linearized form of the Langmuir isotherm, plotting C_e/q_e versus C_e. The linear relationship in this graph confirms the applicability of the Langmuir model to the experimental data [8]. From this plot, key Langmuir parameters such as q_{max} (176.1219 mg/g) and K_L (2.0842 L/mg) were calculated. The high correlation coefficient ($R^2 = 0.9992$) underscores the strong agreement between the Langmuir model and the experimental results, suggesting homogeneity of the adsorption sites. The higher K_L value reflects a strong affinity of CG-AC for MB molecules, confirming its effectiveness as an adsorbent.

The Freundlich isotherm model accounts for the heterogeneity of adsorption sites and the exponential distribution of adsorption energies across the surface. **Figure 7(a)** presents the nonlinear Freundlich isotherm curve, which illustrates the relationship between q_e and C_e. Unlike the Langmuir isotherm, the Freundlich curve does not show a saturation point, indicating the presence of multilayer adsorption on heterogeneous sites with varying energy levels. **Figure 7(b)** shows the linearized Freundlich plot of ln q_e versus ln C_e. The slope and intercept of this plot were used to calculate the Freundlich parameters n and K_F. The Freundlich constant K_F = 124.894 L/g reflects a high adsorption capacity, while the value of n=8.738 confirms favourable adsorption, as n > 1 indicates effective adsorbent-adsorbate interactions. The strong correlation coefficient (R^2 = 0.9982) supports the suitability of the Freundlich model, particularly in describing adsorption behaviour on a heterogeneous surface. However, the slightly lower R^2 compared to the Langmuir model suggests that the latter is a better representation of MB adsorption onto CG-AC.

The Temkin isotherm model considers the impact of adsorbent-adsorbate interactions and assumes that the heat of adsorption decreases linearly with coverage due to adsorbate-adsorbent repulsions. **Figure 8(a)** displays the nonlinear Temkin isotherm curve, showing the variation of q_e with ln C_e. The shape of the curve reflects the energy variation involved in the adsorption process [8, 9]. **Figure 8(b)** illustrates the linearized Temkin plot, where q_e is plotted against ln C_e. The slope and intercept of this graph were used to determine the Temkin constants B_T and K_T. The constant B_T = 15.55 J/mol indicates an exothermic adsorption process, while the equilibrium binding constant K_T = 3477.6 L/g reflects strong adsorbate-adsorbent interactions. Despite the slightly lower correlation coefficient (R^2 = 0.9881) compared to the Langmuir and Freundlich models, the Temkin model provides valuable insights into the energy dynamics of the adsorption process.

Table 2 summarizes the isotherm parameters derived from the Langmuir, Freundlich, and Temkin models. The Langmuir model exhibits the highest correlation coefficient (R^2 = 0.9992), indicating its superior fit to the experimental data. The q_{max} value of 176.1219 mg/g highlights the high adsorption capacity of CG-AC for MB, confirming the suitability of the Langmuir model for describing the adsorption process. The Freundlich model also demonstrates a good fit (R^2 = 0.9982) and emphasizes the role of surface heterogeneity, with K_F = 124.894 and n = 8.738 indicating favorable multilayer adsorption. The Temkin model, while slightly less fitting (R^2 = 0.9881), provides additional insights into the exothermic nature of the adsorption process and energy interactions. In conclusion, the Langmuir model best represents the adsorption of MB onto CG-AC, with strong support from the Freundlich and Temkin models. Together, these models provide a comprehensive understanding of the adsorption mechanism, reinforcing CG-AC's potential as an efficient and reliable adsorbent for dye removal.

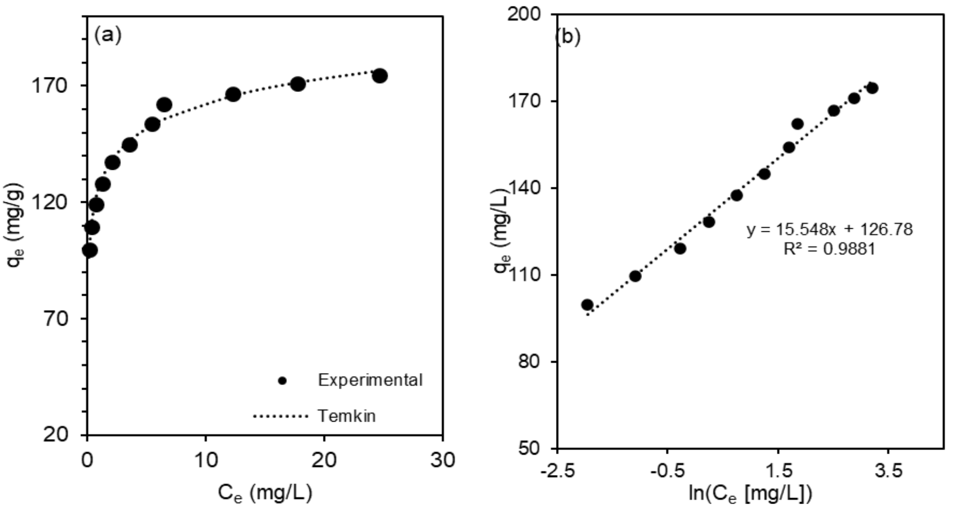

Figure 8. (a) Temkin and (b) Linear Temkin isotherm model for adsorption MB onto CG-AC.

Table 2. Isotherm parameters for the adsorption of MB onto CG-AC.

Langmuir		**Freundlich**		**Temkin**	
q_{max} (mg/g)	176.1219	K_F (I/mg)	124.894	B_T (J/mol)	15.55
K_L (L/mg)	2.0842	n	8.738	K_T (L mg^{-1})	3477.6
R^2	0.9992	R^2	0.9982	R^2	0.9881

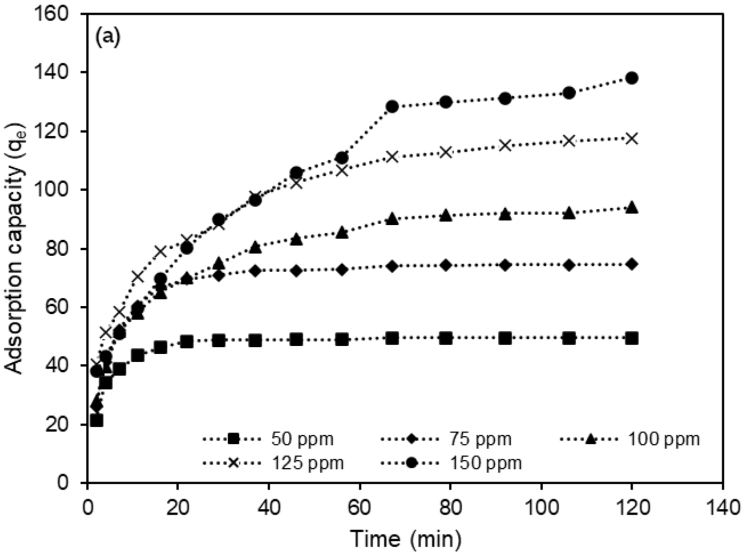

Figure 9. Effect of time and varied MB concentrations on the adsorption capacity of MB.

Kinetic Study

The adsorption of MB onto CG-AC was evaluated over different contact times at varying initial concentrations (50 – 150 mg/L). The results (**Figure 9**) indicate a rapid initial adsorption phase due to the abundance of vacant active sites on CG-AC's surface, followed by a slower phase as these sites become occupied. Equilibrium was reached within 120 minutes for all concentrations, indicating that the adsorption rate depends on concentration. Higher MB concentrations showed greater adsorption capacities due to the increased driving force for mass transfer, consistent with findings in similar studies on MB adsorption using maize silk powder [17].

The PFO model, which assumes that the adsorption rate depends on the availability of unoccupied adsorption sites, was applied. **Figure 10** shows the linear plots of ln (q_e–q_t) versus t revealed poor linearity, with R^2 values ranging from 0.948 to 0.988. Furthermore, the calculated q_e values deviated significantly from the experimental q_e values, as shown in Table 2. These discrepancies suggest that the PFO model inadequately describes the adsorption process, aligning with observations from studies where chemisorption mechanisms dominated over physisorption as reported by Handayani et al. [18].

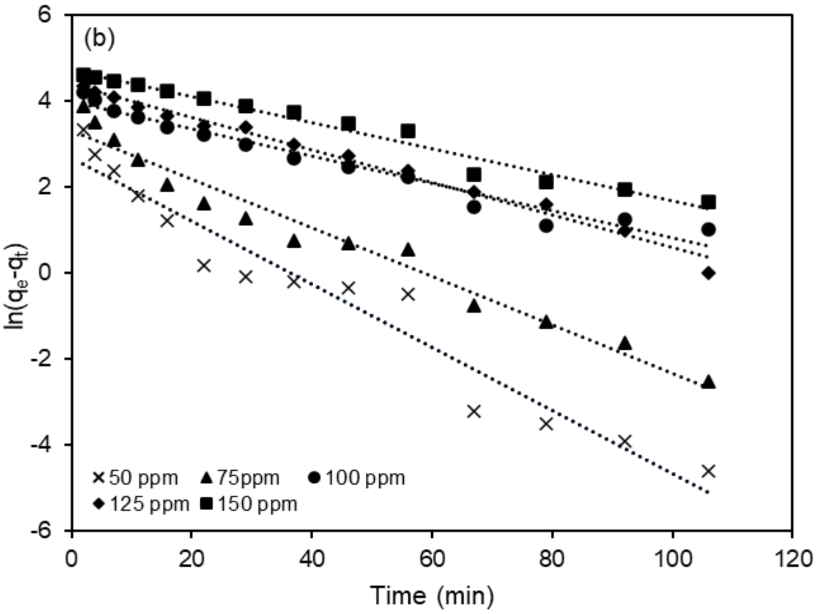

Figure 10. PFO model for the adsorption of MB to CG-AC.

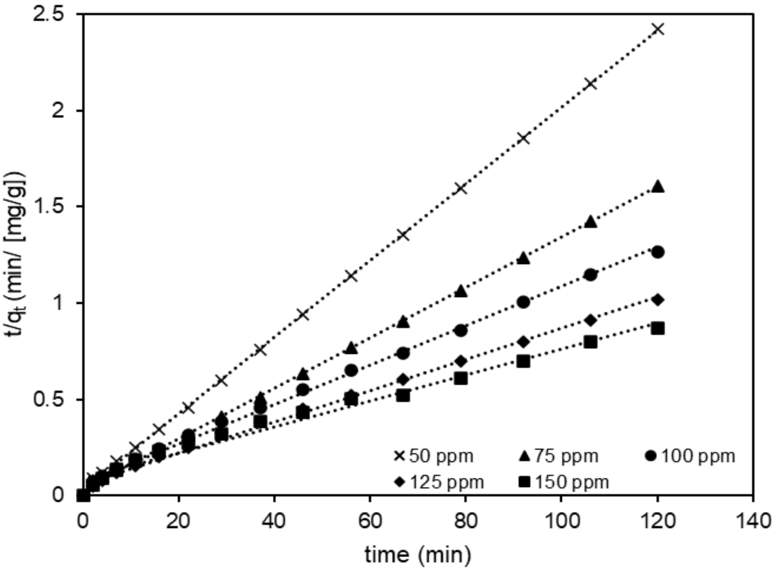

Figure 11. PSO model for the adsorption of MB to CG-AC.

The PSO model is depicted in **Figure 11**, which is based on chemisorption involving electron sharing or exchange between the adsorbent and adsorbate and showed superior performance. The plots of t/q_t versus t yielded R^2 values exceeding 0.99, indicating excellent linearity. Moreover, the calculated q_e values closely matched the experimental data (**Table 3**). These results confirm that the adsorption process follows PSO kinetics, consistent with similar studies on MB adsorption using polydopamine microspheres [19]. The dominance of PSO kinetics implies that chemical interactions, such as hydrogen bonding or π-π stacking, play a crucial role in MB adsorption.

The IPD model was evaluated from **Figure 12** to explore the diffusion mechanism. The multi-linearity observed in the plots of q_t versus $t^{1/2}$ suggests a three-stage adsorption process: (1) external surface adsorption, (2) gradual adsorption involving intraparticle diffusion, and (3) equilibrium. The diffusion rate constants (k_{ID}) and intercepts (C) are summarized in **Table 3**. Higher MB concentrations yielded larger k_{ID} values, indicating faster diffusion rates. However, the non-zero C values and moderate R^2 values (0.383 – 0.885) reveal that intraparticle diffusion is not the sole rate-limiting step, in agreement with findings by Shin and Kim [20].

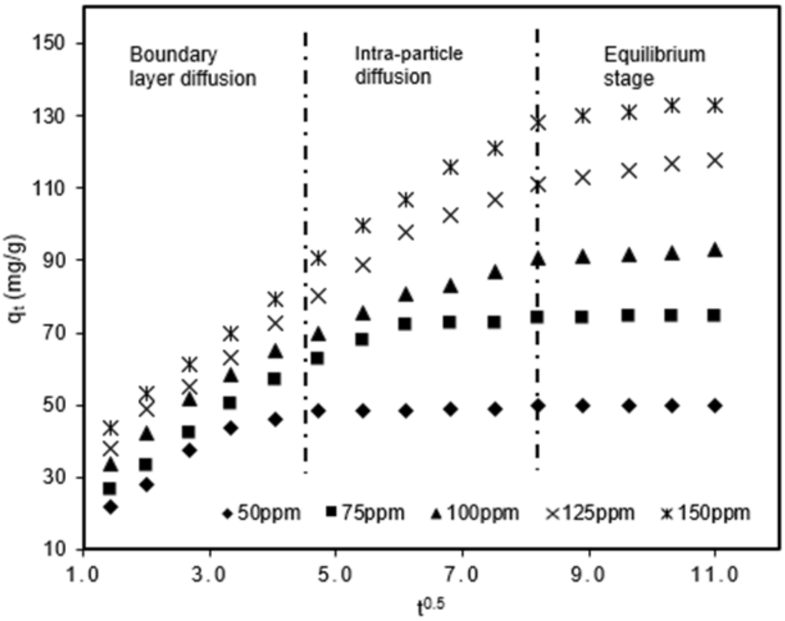

Figure 12. IPD model for the adsorption of MB to CG-AC.

Comparative analysis of the three models demonstrates that the PSO model provides the best fit for the adsorption data, as evidenced by the high R^2 values and the agreement between q_e (calculated) and q_e (experimental) values. While the PFO model failed to accurately describe the process, the IPD model revealed the involvement of multiple adsorption stages but could not independently govern the kinetics. These findings are consistent with literature reports that highlight PSO kinetics for adsorption systems dominated by chemisorption mechanisms, such as those involving activated carbons from corn husk [18]. This comprehensive kinetic study elucidates the adsorption mechanism of MB onto CG-AC, confirming chemisorption as the primary pathway and providing valuable insights for optimizing the design of wastewater treatment systems.

Thermodynamic Study

The thermodynamic analysis provides significant insights into the nature and feasibility of the adsorption process of MB onto CG-AC. The slope and intercept of the Van't Hoff plot, which correlates ln K_D with 1/T (**Figure 13**), were utilized to determine the enthalpy change (ΔH°) and entropy change (ΔS°), respectively. Subsequently, these values were employed to calculate the Gibbs free energy change (ΔG°) at various temperatures.

Table 3. Parameters of PFO, PSO and IPD kinetics model.

Concentration (mg/L)	$q_{e\,(exp)}$	PFO			PSO		
		$q_{e\,(calc)}$	K_{ad}	R^2	$q_{e\,(calc)}$	k_2	R^2
50	49.5	14.5	0.011844	0.948	50.4648	0.011844	0.9998
75	74.5	27.7	0.004567	0.966	76.71154	0.004567	0.9995
100	94.9	53.1	0.001313	0.962	99.50703	0.001313	0.9967
125	117.7	79.5	0.00096	0.988	124.7598	0.00096	0.9955
150	138.2	111.9	0.000411	0.976	152.7035	0.000411	0.9560

Concentration (mg/L)	IPD		
	k_{ID}	C	R^2
50	0.1267	39.168	0.3834
75	0.2520	53.473	0.4556
100	0.4585	51.994	0.7310
125	0.5805	63.544	0.7854
150	0.8526	54.299	0.8854

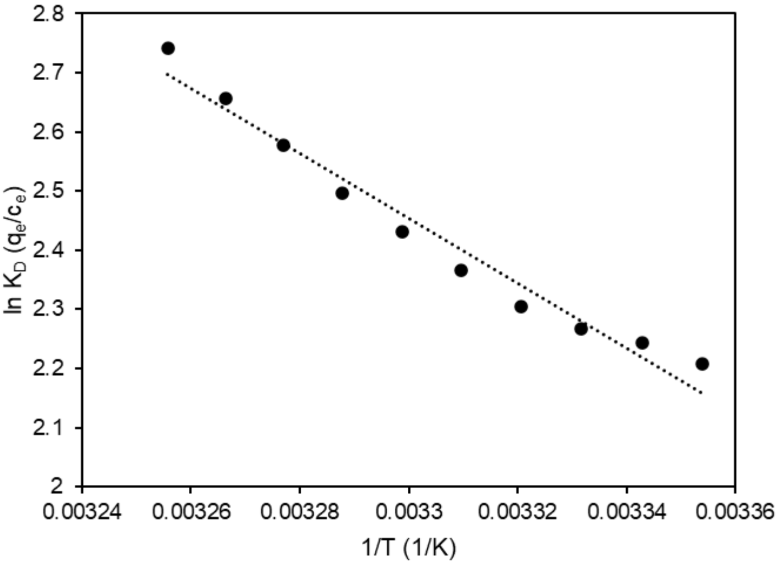

Figure 13. Thermodynamic Van't Hoff plot.

Table 4. Thermodynamic study for adsorption.

Temperature °C	**K_{ad} (L/g)**	**ΔG° (kJ/mol)**	**ΔH° (kJ/mol)**	**ΔS° (J/mol.K)**
25	9.09	-5.47	45.58	170.83
26	9.42	-5.55		
27	9.65	-5.65		
28	10.02	-5.77		
29	10.65	-5.94		
30	11.36	-6.12		
31	12.13	-6.31		
32	13.16	-6.53		
33	14.25	-6.76		
34	15.51	-7.00		

The calculated ΔG° values, which ranged from -5.47 kJ/mol to -7.00 kJ/mol as the temperature increased from 25 °C to 43 °C (Table 4), were negative, indicating that the adsorption process was spontaneous. This trend of more negative ΔG° values at elevated temperatures indicates that the spontaneity of adsorption diminishes as temperature increases. This observation aligns with the findings of Ouaddari et al. [8], who reported similar trends for MB adsorption on natural and purified clays, confirming that higher temperatures slightly reduce the thermodynamic favorability of adsorption.

The enthalpy change (ΔH°) was determined to be 45.58 kJ/mol (**Table 4**), indicating that the process is endothermic. Endothermic adsorption processes, such as those reported by Handayani et al. [18], typically involve physical or chemical interactions requiring energy input, which corroborates the strong affinity observed between CG-AC and MB molecules. Furthermore, the magnitude of ΔH° is within the range of chemisorption processes, suggesting that the adsorption mechanism likely involves stronger adsorbent-adsorbate interactions than physisorption alone.

The entropy change (ΔS°) values were found to be positive, signifying an increase in randomness at the adsorbent-adsorbate interface during the adsorption process. This finding is consistent with the results of Miraboutalebi et al. [17], who observed that positive ΔS° values indicate the structural rearrangement of adsorbed molecules and enhanced system disorder. Such behavior is typical in adsorption systems where the dye molecules interact dynamically with activated carbon's functional groups, as noted by Iqajtaoune et al. [12].

In conclusion, the thermodynamic study underscores that MB adsorption onto CG-AC is spontaneous, endothermic, and characterized by a significant degree of adsorbate-adsorbent interaction. These results not only align with previous studies on similar systems but also highlight CG-AC's efficacy as a sustainable adsorbent for dye removal under variable thermal conditions.

CONCLUSION

This study demonstrates the potential of coffee ground-derived activated carbon (CG-AC) as an effective adsorbent for methylene blue (MB) removal from water. Adsorption efficiency was influenced by pH, initial concentration, contact time, and temperature, with higher pH favoring adsorption due to electrostatic interactions. Increasing MB concentration enhanced adsorption capacity, and equilibrium was reached within a defined time frame, emphasizing the significance of contact time. Kinetic analysis revealed the pseudo-second-order (PSO) model as the best fit, indicating chemisorption as the primary mechanism. The intraparticle diffusion (IPD) model confirmed that adsorption occurred through a multi-step process, involving external surface adsorption, intraparticle diffusion, and equilibrium. Equilibrium data were well-described by Langmuir, Freundlich, and Temkin isotherms, with the Langmuir model yielding the best fit and a maximum monolayer adsorption capacity of 176.12 mg/g. Thermodynamic parameters confirmed a spontaneous and endothermic process, as indicated by negative Gibbs free energy (ΔG°) values (-5.47 to -7.00 kJ/mol) and positive enthalpy (ΔH° = 45.58 kJ/mol) and entropy (ΔS° = 170.83 J/mol·K) changes. These results underscore the efficiency of CG-AC in MB removal, providing a deeper understanding of adsorption mechanisms and optimization parameters. This study highlights CG-AC as a sustainable and cost-effective solution for mitigating dye contamination in textile industry wastewater, contributing valuable insights for the development of improved wastewater treatment technologies.

ACKNOWLEDGEMENTS

This research was supported by Universiti Teknologi MARA (UiTM), whose resources and facilities were instrumental in the successful completion of this work. We extend our heartfelt gratitude to the Ministry of Higher Education (MOHE) for their generous financial support, continuous encouragement, and commitment to advancing academic research. Their invaluable contributions provided the foundation for this study, and we deeply appreciate their role in fostering innovation and excellence in our research endeavors.

REFERENCES

1. Pandey, D., Daverey, A., Dutta, K., Yata, V. K. and Arunachalam, K. (2022) Valorization of waste pine needle biomass into biosorbents for the removal of methylene blue dye from water: Kinetics, equilibrium and thermodynamics study. *Environmental Technology & Innovation*, **25**, 102200.

2. Aragaw, T. A. and Alene, A. N. (2022) A comparative study of acidic, basic, and reactive dyes adsorption from aqueous solution onto kaolin adsorbent: Effect of operating parameters, isotherms, kinetics, and thermodynamics. *Emerging Contaminants*, **8**, 59–74.

3. Soni, S., Bajpai, P. K., Mittal, J. and Arora, C. (2020) Utilisation of cobalt doped Iron based MOF for enhanced removal and recovery of methylene blue dye from waste water. *Journal of Molecular Liquids*, **314**, 113642.

4. Teymur, Y. A. and Güzel, F. (2023) Ultra-efficient removal of methylene blue, oxytetracycline, and lead(II) by activated carbon derived from black cumin (*Nigella sativa*) processing solid waste. *Journal of Water Process Engineering*, **54**, 103940.

5. Veeraragavan, A. J., Shanmugavel, R., Abraham, N., Subramanian, D. and Pandian, S. (2021) Kinetic studies validated by Artificial Neural Network simulation for the removal of dye from simulated waste water by the activated carbon produced from Acalypha indica leaves. *Environmental Technology & Innovation*, **21**, 101244.

6. Deivasigamani, P., Kumar, P. S., Sundaraman, S., Soosai, M. R., Renita, A. A., Karthikeyan, M., Bektenov, N., Baigenzhenov, O., Venkatesan, D. and Kumar, A. (2023) Deep insights into kinetics, optimization and thermodynamic estimates of methylene blue adsorption from aqueous solution onto coffee husk (*Coffee arabica*) activated carbon. *Environmental Research*, **236**, 116735.

7. Mani, D., Elango, D., Priyadharsan, A., Al-Humaid, L. A., Al-Dahmash, N. D., Ragupathy, S., Jayanthi, P. and Ahn, Y. H. (2023) Groundnut shell chemically treated with KOH to prepare inexpensive activated carbon: Methylene blue adsorption and equilibrium isotherm studies. *Environmental Research*, **231**, 116026.

8. Ouaddari, H., Abbou, B., Lebkiri, I., Habsaoui, A., Ouzzine, M. and Allah, R. F. (2024) Removal of Methylene Blue by adsorption onto natural and purified clays: Kinetic and thermodynamic study. *Chemical Physics Impact*, **8**, 100405.

9. Daniel, L. S., Rahman, A., Hamushembe, M. N., Kapolo, P., Uahengo, V. and Jonnalagadda, S. B. (2023) The production of activated carbon from *Acacia erioloba* seedpods via phosphoric acid activation method for the removal of methylene blue from water. *Bioresource Technology Reports*, **23**, 101568.

10. Chen, J., Li, J., Zeng, Q., Li, H., Chen, F., Hou, H. and Lan, J. (2022) Efficient removal of tetracycline from aqueous solution by Mn-N-doped carbon aerogels: Performance and mechanism. *Journal of Molecular Liquids*, **358**, 119153.

11. Kim, Y. S. and Kim, J. H (2019) Isotherm, kinetic and thermodynamic studies on the adsorption of paclitaxel onto Sylopute. *The Journal of Chemical Thermodynamics*, **130**, 104–113.

12. Iqajtaoune, A., Taibi, M. H., Saufi, H., Aouan, B. and Boudad, L. (2024) Enhanced removal of methylene blue and procion deep red H-EXL dyes from aqueous environments by modified-bentonite: Isotherm, kinetic, and thermodynamic. *Desalination and Water Treatment*, **320**, 100607.

13. Wardighi, Z., Bensalah, J., Zarrouk, A. and Lebkiri, A. (2023) Investigation of adsorption and mechanism of the cationic methylene blue by the polymeric *Rubia tinctorum* seeds from environment wastewater: kinetic equilibrium and thermodynamic studies. *Desalination and Water Treatment*, **310**, 212–225.

14. Hazzaa, R. and Hussein, M. (2015) Adsorption of cationic dye from aqueous solution onto activated carbon prepared from olive stones. *Environmental Technology & Innovation*, **4**, 36–51.

15. Joshiba, G. J., Kumar, P. S., Rangasamy, G., Ngueagni, P. T., Pooja, G., Balji, G. B., Alagumalai, K. and El-Serehy, H. A. (2022) Iron doped activated carbon for effective removal of tartrazine and methylene blue dye from the aquatic systems: Kinetics, isotherms, thermodynamics and desorption studies. *Environmental Research*, **215**, 114317.

16. Al-Ghouti, M. A. and Da'ana, D. A. (2020) Guidelines for the use and interpretation of adsorption isotherm models: A review. *Journal of Hazardous Materials*, **393**, 122383.

17. Miraboutalebi, S. M., Nikouzad, S. K., Peydayesh, M., Allahgholi, N., Vafajoo, L. and McKay, G. (2017) Methylene blue adsorption via maize silk powder: Kinetic, equilibrium, thermodynamic studies and residual error analysis. *Process Safety and Environmental Protection*, **106**, 191–202.

18. Handayani, T., Ramadhani, P. and Zein, R. (2024) Modelling studies of methylene blue dye removal using activated corn husk waste: Isotherm, kinetic and thermodynamic evaluation. *South African Journal of Chemical Engineering*, **47**, 15–27.

19. Fu, J., Chen, Z., Wang, M., Liu, S., Zhang, J., Zhang, J., Han, R. and Xu, Q. (2015) Adsorption of methylene blue by a high-efficiency adsorbent (polydopamine microspheres): Kinetics, isotherm, thermodynamics and mechanism analysis. *Chemical Engineering Journal*, **259**, 53–61.

20. Shin, H. S. and Kim, J. H. (2016) Isotherm, kinetic and thermodynamic characteristics of adsorption of paclitaxel onto Diaion HP-20. *Process Biochemistry*, **51(7)**, 917–924.